Initiated Chemical Vapor Deposition (iCVD) of Poly(alkyl acrylates): A Kinetic Model

Kenneth K. S. Lau* and Karen K. Gleason*

Department of Chemical Engineering, Massachusetts Institute of Technology, 77 Massachusetts Avenue, Cambridge, Massachusetts 02139

Received January 23, 2006; Revised Manuscript Received March 9, 2006

ABSTRACT: In a two-part investigation, an experimental study and a kinetic model analysis of the initiated chemical vapor deposition (iCVD) of alkyl acrylate polymers are described. In this second part, a kinetic model was developed to examine the reaction mechanisms of iCVD polymerization. The model incorporated surface polymerization events of initiation, propagation, and termination as well as primary radical termination and recombination. By using a multiresponse parameter estimation procedure based on minimizing a determinant criterion, the model fitted closely to experimental data on butyl acrylate iCVD that measured the effect of a change in monomer surface concentration on both the rate of polymerization and polymer molecular weight. Model propagation and termination rate coefficients, 15 540 and 0.98×10^6 L/mol·s, respectively, matched well with those of liquid-phase butyl acrylate radical polymerization, 15 460 and 10^6 L/mol·s, respectively. The model captured the linear dependencies of rate and molecular weight to monomer concentration typical of liquid-phase radical polymerization. At low concentrations, the model further captured the nonlinear rate behavior, which was attributed to significant primary radical termination. Sensitivity analysis revealed a well-behaved model with model parameters that trended realistically. These results provided strong support for a surface-driven iCVD polymerization that is surprisingly analogous to bulk-phase free radical polymerization. A proven iCVD kinetic model would ultimately facilitate process scale-up and provide a priori predictions on the feasibility of new iCVD chemistries.

Introduction

Polymer films and coatings made by initiated chemical vapor deposition (iCVD) are shown to produce clean, stoichiometric polymer compositions, e.g., poly(tetrafluoroethylene),[1] poly(glycidyl methacrylate),[2] poly(2-hydroxyethyl methacrylate),[3] poly(methyl methacrylate),[4] and poly(perfluoroalkylethyl methacrylate).[5] Essentially, iCVD can be considered a free radical polymerization without the use of a liquid phase, conveniently combining polymerization and coating in a single, all-dry step. It involves the vapor-phase delivery of initiator and monomer into a vacuum chamber maintained at a pressure typically between 10^{-1} and 1 Torr, thermal activation of the initiator vapor using filament wires heated to a temperature typically in the range of 200 to 400 °C, and subsequent polymerization of monomer from activated radicals on a surface, which is kept at a much lower temperature, typically less than 50 °C, to promote adsorption. As illustrated in Figure 1, the mechanism of iCVD polymerization is believed to occur through three major steps: (1) thermal decomposition of an initiator in the vapor phase to form primary radicals, (2) diffusion and adsorption of primary radicals and monomer from the vapor phase onto a surface, and (3) polymerization of monomer on the surface via initiation, propagation, and termination events to form a continuous polymer coating.

Although iCVD may appear similar to vapor deposition polymerization of parylene,[6] it is distinct in that an initiator is used to create the active radicals rather than through high-temperature pyrolysis of the deposition precursor, which, in the parylene deposition, is the parylene ring dimer. iCVD may be closer to vapor deposition polymerization reported for some vinyl monomers such as methacrylates and styrenes.[7−15] However, in contrast to iCVD, these reports relied on either a heated substrate,[7] putting an initiator on the surface prior to polymerization,[8−10] photoactive initiation,[11−13] or an extremely hot filament but without any initiator to produce the active radicals necessary for polymerization.[14,15] There have been attempts to model the kinetics of parylene polymerization to explain observed rate phenomena.[16,17] A mechanism was also proposed for the vinyl monomer deposition polymerization using a surface initiator, although no quantitative model was developed to describe the experimental results.[9]

The aim of this paper is to formulate a mathematical model to describe iCVD kinetic data. Experimentally, as detailed in the preceding paper,[18] kinetics of iCVD polymerization were found to be strongly adsorption-limited, with monomer concentration at the surface being an important rate determinant. A homologous series of alkyl acrylates, from ethyl to hexyl acrylate, that were iCVD polymerized showed higher polymer deposition rate and molecular weight with a heavier monomer, suggesting that kinetics were enhanced by greater monomer adsorption from the less volatile monomer at equal gas concentrations. Further analysis with ethyl acrylate iCVD polymerization showed that a decrease in substrate temperature yielded significantly higher deposition rates, with an apparent negative activation energy that was quantitatively related to the heat of desorption, indicating again that greater monomer adsorption produced faster kinetics. Additionally, the dependence of rate on monomer surface concentration was similar to that observed in certain liquid-phase radical polymerizations. Thus, in this paper, an iCVD kinetic model, based on the surface-driven radical polymerization reaction mechanism proposed in Figure 1, was mathematically developed to help understand the experimentally observed rate behavior. Ultimately, a quantitative grasp on iCVD mechanistics would aid in scaling the iCVD process beyond simply a research novelty and, ideally, enable a priori predictions of the feasibility of new iCVD chemistries.

* Corresponding authors. E-mail: klau@mit.edu (K.K.S.L.); kkg@mit.edu (K.K.G.).

10.1021/ma0601621 CCC: $33.50
Published on Web 04/11/2006

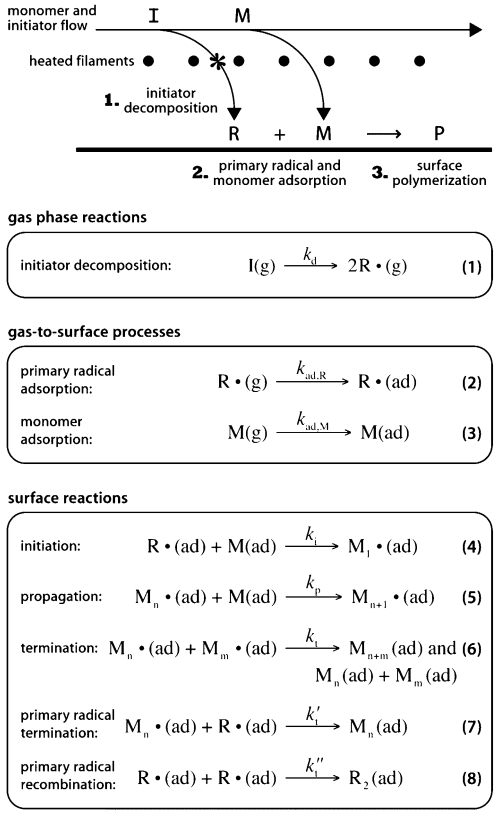

Figure 1. Reaction mechanism proposed for iCVD polymerization. Initiator is thermally decomposed in the vapor phase in the vicinity of the heated filaments to form primary radicals (**1**). Primary radicals diffuse to the surface and become adsorbed (**2**). Monomer is also adsorbed from the vapor phase onto the surface (**3**). Polymerization is initiated at the surface by the attack of a primary radical on a monomer molecule (**4**). Polymerization is propagated by the addition of more monomer units (**5**). Polymerization is terminated by bimolecular chain termination through coupling or disproportionation (**6**). Polymer chains can also terminate by primary radical termination through the attack of a primary radical on a polymer radical (**7**). Primary radicals can also recombine with each other (**8**).

Model Development

As outlined in Figure 1, the reaction mechanism proposed for iCVD polymerization can be broken down into a sequence of reaction steps. The main reaction occurring in the gas phase is believed to be the thermal decomposition of the initiator around the vicinity of the heated filaments to form primary radicals (**1**). In the case of *tert*-amyl peroxide as the initiator, thermal decomposition initially yields the *tert*-amyl peroxyl radical. However, experimentally, it is found that this peroxyl radical rapidly undergoes β-scission to form acetone and an ethyl radical.[19−21] It is therefore quite probable that the ethyl radical would be the primary radical in this specific case, and consequently, primary radical recombination would not reform the initiator molecule. Because the thermal zone where primary radicals are generated is some distance away from the surface, these radicals necessarily have to diffuse to the surface before they are adsorbed (**2**). Monomer, on the other hand, is delivered into the iCVD reactor continuously and in sufficient gas-phase concentrations that equilibrium conditions are expected for its adsorption onto the surface (**3**). With primary radicals and monomer on the surface, polymerization occurs through reaction pathways of initiation (**4**), propagation (**5**), and termination (**6**) analogous to liquid-phase free radical polymerization. Because experimental evidence from the first paper suggests that there could be a high concentration of primary radicals under certain process conditions, included also are primary radical termination (**7**) and recombination (**8**) processes that come into play when these radicals become appreciable.

As is evident, all the surface reactions in iCVD polymerization are identical to the radical polymerization steps in the bulk phase, albeit on a surface. Thus, the kinetic equations from bulk-phase radical polymerization can be directly applied to iCVD polymerization *if only surface events are considered* in the model. The two main kinetic equations describing radical polymerization are then the rate of polymerization, R_p, and the kinetic chain length, ν:

$$R_p = -\frac{d[M]}{dt} = k_p[M][M\bullet] \tag{1}$$

$$\nu = \frac{R_p}{R_i} = \frac{k_p[M][M\bullet]}{k_i[M][R\bullet]}; \qquad X_n = \frac{2\nu}{(2-a)}; \qquad M_n = MW_M X_n \tag{2}$$

where [M] is the monomer concentration, [M•] is the polymer radical concentration, and [R•] is the primary radical concentration. Given also in eq 2 are the relationships to derive the number-average degree of polymerization, X_n, and the number-average molecular weight, M_n. The parameter a reflects the fraction of polymer radicals that terminate by coupling, $(1 - a)$ being the fraction terminating by disproportionation, while MW_M is the molar mass of the polymer repeat unit. Detailed derivation and the underlying assumptions of eqs 1 and 2 can be found in Odian.[22]

Equations 1 and 2 are intractable in their present form, as it is practically impossible to measure radical concentrations experimentally. This difficulty can be circumvented by using a steady-state approximation, analogous to bulk-phase radical polymerization,[22] in which primary radical and polymer radical concentrations on the surface are assumed to be constant. Mass balances can then be written for [R•] and [M•]:

$$[R\bullet]\ \text{balance:}\ \ r = k_i[M][R\bullet] + k_t'[M\bullet][R\bullet] + 2k_t''[R\bullet]^2 \tag{3}$$

$$[M\bullet]\ \text{balance:}\ \ k_i[M][R\bullet] = 2k_t[M\bullet]^2 + k_t'[M\bullet][R\bullet] \tag{4}$$

where r is a parameter introduced to represent the rate of "appearance" of primary radicals on the surface. The mechanism given in Figure 1 indicates that r is equal to the rate of primary radical adsorption (**2**). However, it must be noted that, within the confines of the steady-state approximation cast in eq 3, r represents only the rate of primary radicals adsorbed that eventually gets consumed by surface reactions, specifically by (**4**), (**7**), and (**8**). It ignores primary radicals adsorbed that may be lost through other reactions or sinks not considered in Figure 1, and thus, r does not necessarily reflect the total rate of primary radical adsorption as (**2**) seems to imply. Nevertheless, setting r as a fitting parameter conveniently precludes the need to mathematically describe gas-phase initiator dissociation and subsequent primary radical diffusion, which in the case of iCVD, is expected to be quite complex because there is inevitably a thermal gradient surrounding each heated filament, leading to spatial variations in the rate of initiator decomposition and also temperature-dependent diffusion that cannot be defined simply. More significantly, defining the parameter r allows solely surface reactions to be considered, hence enabling the use of bulk-phase kinetic equations in a simple manner.

Being implicit in [R•] and [M•], eqs 3 and 4 can be solved simultaneously to obtain expressions for [R•] and [M•]. These expressions can then be substituted for [R•] and [M•] in eqs 1 and 2 to yield the general form of the iCVD kinetic model

Table 1. Experimental Conditions and Kinetic Measurements of Butyl Acrylate iCVD

$F_{monomer}$[a] (sccm)	$F_{initiator}$[b] (sccm)	F_{argon} (sccm)	P (Torr)	$T_{substrate}$ (°C)	$T_{filament}$ (°C)	P_M/P_{sat}[c]	DR (nm/min)	M_n (g/mol)
3.00	0.70	0.00	1.0	23	260	0.1673	46.8	15 200
2.50	0.58	0.62	1.0	23	260	0.1394	36.6	12 700
2.00	0.47	1.23	1.0	23	260	0.1115	26.1	10 400
1.50	0.35	1.85	1.0	23	260	0.0837	15.3	7800
1.00	0.23	2.47	1.0	23	260	0.0558	7.9	4200
0.75	0.18	2.77	1.0	23	260	0.0418	4.0	3700
0.50	0.12	3.08	1.0	23	260	0.0279	1.7	2300

[a] Monomer is *n*-butyl acrylate. [b] Initiator is *tert*-amyl peroxide. [c] $P_M = (F_M/F_{total})P$; $P_{sat} = 4.85$ Torr at 23 °C.

relating rate of polymerization, R_p, and number-average molecular weight, M_n, to monomer concentration, [M], together with seven unknown parameters: k_i, k_p, k_t, k_t', k_t'', r, and a. The model assumes the rate coefficients are independent of chain length of the growing polymer radicals for simplicity, although it is recognized that there may be chain length dependencies, especially with termination rate coefficient at least pertaining to bulk-phase polymerization.[23,24] This may lead to a less accurate description of the molecular weight distribution (MWD) because all the possible termination events of polymer radicals of different chain lengths are essentially lumped into this single-weighted average rate coefficient,[25] although, for the present case, this is inconsequential because MWD has not been considered in developing the model. The model also ignores any transfer processes by which a propagating chain gives up its radical site to another molecule. As given by the Mayo equation, chain transfer processes usually lead to a lower degree of polymerization and molecular weight than if only bimolecular chain termination were considered.[22] By ignoring chain transfer, it is possible that the present model may overestimate molecular weight. However, with iCVD, many of the transfer processes are either absent or relatively negligible. There is no transfer to solvent. Any transfer to initiator is expected to be minimal because surface adsorption of the initiator is expected to be much less relative to the monomer and primary radicals given that the initiator is generally much more volatile in iCVD. In liquid-phase radical polymerization, transfer to monomer is generally small, while transfer to polymer is considered minor even at high conversions,[22] so these are assumed to be similarly inconsequential in iCVD. With iCVD, there is the additional possibility of transfer to the substrate. However, this would only occur, if significantly, during the initial stages of polymer deposition when the growing chains are in the immediate vicinity of the substrate. With sufficient thickness of the polymer layer, the propagating chains should no longer be influenced by the underlying substrate.

Experimental Section

To relate the iCVD kinetic model to experimental data, an experiment was designed to study the iCVD polymerization of butyl acrylate, specifically looking at the effect of changing monomer surface concentration on polymer deposition rate and molecular weight. To alter the monomer concentration at the surface in the most straightforward way, partial pressure of the monomer, P_M, was varied while keeping all other depositions conditions constant. Without a change in substrate or filament temperature, reaction rate coefficients were expected to remain more or less constant. A change in kinetics would therefore be wholly a result of a change in monomer surface concentration, which can be related back to monomer partial pressure by the P_M/P_{sat} ratio expressed through the Brunauer−Emmett−Teller or BET adsorption equation,[26] where the monomer-saturated vapor pressure, P_{sat}, remains unchanged at a fixed substrate temperature.

Butyl acrylate was iCVD polymerized at various monomer partial pressures by using argon as the diluent gas. Table 1 summarizes the series of deposition conditions used. Reactor pressure and total gas flow rate were kept constant at 1.0 Torr and 3.70 sccm, respectively, to maintain a constant residence time in the reactor. Initiator and monomer flow rates were kept at a constant ratio of 0.233 to maintain the same relative concentration of reactive precursors. Substrate and filament temperatures were set at 23 and 260 °C, respectively. The *tert*-amyl peroxide initiator and *n*-butyl acrylate monomer were purchased from Aldrich and used as received. Complete details of the iCVD reactor setup and deposition protocol have been described previously.[18]

The thickness of the deposited films was determined using spectroscopic ellipsometry. A J. A. Woollam M-2000S equipped with a mapping stage was used to measure the Ψ and Δ angles at 13 points over the coated silicon wafer. Each point measurement was taken at an incidence angle of 70° and for 190 wavelengths between 315 and 718 nm. The raw data was fitted to a model that consisted of a Cauchy−Urbach layer on top of a silicon substrate with a native oxide surface layer. The derived thicknesses were averaged over all points and deposition rate was calculated as the ratio of average thickness to deposition time. Thickness variations were within 10% for each sample.

The number-average molecular weight of the deposited films was determined using a Waters gel permeation chromatography (GPC) system. For each sample, the film was dissolved off the wafer by washing with tetrahydrofuran (Aldrich) and the polymer solution adequately concentrated before it was injected into the GPC column maintained at 35 °C. The molecular weight was then calculated from the integrated area of the GPC trace through a calibration made with a set of narrow poly(methyl methacrylate) standards of known molecular weight and molecular weight distribution. Although molecular weight distribution is not included in the present iCVD kinetic model, experimental polydispersity indices derived from GPC range between 2 and 3, typical of values obtained from bulk-phase radical polymerization.

To explicitly quantify the concentration of monomer at the surface, separate adsorption experiments were performed using a vacuum-compatible Sycon Instruments quartz crystal microbalance (QCM). The setup had a 16-mm-diameter gold-coated crystal sensor that was maintained at 23 °C. Adsorption caused a frequency shift in the crystal that was directly related to the mass of monomer adsorbed (in $\mu g/cm^2$) according to the Sauerbrey equation.[27] Desorption caused a frequency shift in the opposite direction. The amount of monomer adsorbed was taken as the average of the adsorption and desorption runs because monomer only physisorbed and adsorption was reversible. In one series of runs, butyl acrylate was introduced at a fixed flow rate but at various pressures, while in a second series of runs, total pressure was fixed while butyl acrylate partial pressure was varied by altering gas flow rates with argon added as a diluent.

Results and Discussion

Experimental Data. On the basis of a controlled experiment to determine the effect of a change of monomer partial pressure, P_M, on iCVD kinetics of butyl acrylate, Table 1 lists the resulting polymer deposition rate and number-average molecular weight measured. Figure 2 plots out these results as a function of P_M/P_{sat} ($P_{sat} = 4.85$ Torr at a fixed substrate temperature of 23 °C[28]). The experimental data in Figure 2 is also plotted as a

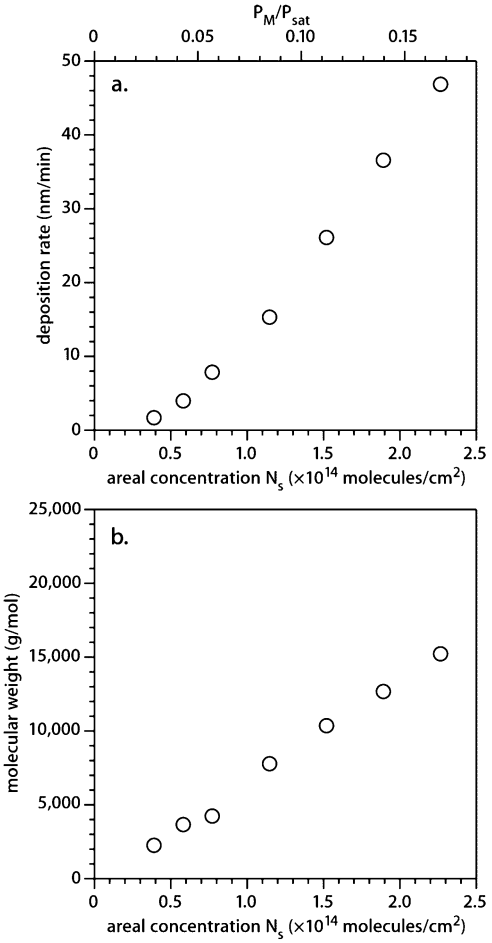

Figure 2. Experimental data showing the effect of a change in monomer surface concentration, indirectly through a change in monomer partial pressure with all other conditions unchanged, on polymer deposition rate (a) and number-average molecular weight (b) for butyl acrylate iCVD polymerization. Plotted as a function of P_M/P_{sat} and N_s, both being direct expressions for monomer surface concentration within the range of conditions considered. There seems to be a linear increase in molecular weight with concentration. Deposition rate shows nonlinear behavior at low monomer concentrations, which appears to become linear at sufficiently high concentrations.

function of the areal concentration of butyl acrylate, N_s, during deposition. The relationship between N_s and P_M/P_{sat} was derived by using the BET equation through separate QCM adsorption measurements of butyl acrylate at 23 °C, see Figure 3. For Figure 3, the raw QCM data in μg/cm^2 was converted to adsorbed volume, V_{ad}, using the liquid density of butyl acrylate ($\rho_M = 0.901$ g/cm^3) and QCM sensor area ($A_{QCM} = 2.011$ cm^2), while the raw data was converted to N_s based on the molar mass of butyl acrylate ($MW_M = 128$ g/mol).

As seen in Figure 3, changes in total pressure or partial pressure of the monomer gave similar adsorption behavior. In fact, a single BET equation[29] (eq 5) can be fitted to both sets of data to yield the fitted constants V_{ml} and c as 265.0 pL and 2.536, respectively ($R^2 = 0.9951$).

$$V_{ad} = \frac{V_{ml}c(P_M/P_{sat})}{(1 - P_M/P_{sat})[1 - (1 - c)(P_M/P_{sat})]} \qquad (5)$$

Figure 3 also reveals that, at P_M/P_{sat} ratios below 0.2, monomer surface concentration is linearly proportional to P_M/P_{sat}. Looking at Table 1, the deposition conditions for the series of iCVD polymerized butyl acrylate were below this limit. Further, deposition conditions were also well below the areal concentration

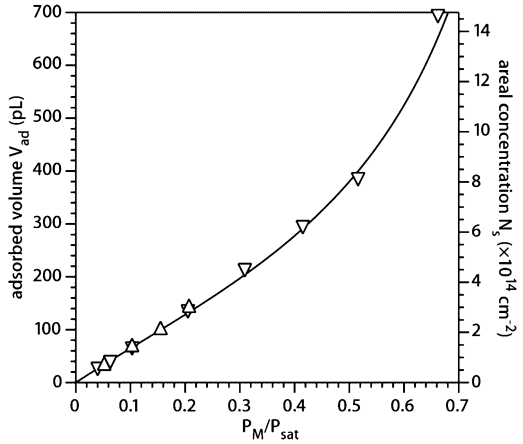

Figure 3. QCM adsorption measurements of butyl acrylate at 23 °C. The raw data was converted from μg/cm^2 to adsorbed volume, V_{ad}, in pL, using the liquid density of butyl acrylate (0.901 g/cm^3) and QCM sensor area (2.011 cm^2). The data were also converted to areal concentration of butyl acrylate, N_s, in molecules/cm^2, using its molar mass (128 g/mol). Measurements are shown for a change in total monomer pressure (▽) without diluent and for a change in partial pressure (△) at constant total pressure, using argon as diluent. A single BET equation can be fitted to all the data ($R^2 = 0.9951$), from which the values of the fitted parameters V_{ml} and c are 265.0 pL and 2.536, respectively.

of 5.59×10^{14} cm^{-2} for a monolayer coverage, this value being derived from the adsorbed volume of a full monolayer, V_{ml}, reached at P_M/P_{sat} of 0.386. Thus, for this experimental series, P_M/P_{sat} can be viewed as a *direct* measure of monomer surface concentration.

Going back to Figure 2 then, qualitatively, the observed molecular weight shows a nearly linear increase with monomer surface concentration. The observed deposition rate also shows an apparently linear increase at sufficiently high surface concentrations. Interestingly, these linear trends with monomer concentration are generally observed in liquid-phase radical polymerization as well.[22] The nonlinear dependence of deposition rate at low concentrations may be similar to that observed for iCVD of ethyl acrylate discussed in the preceding paper and may be due to significant primary radical termination affecting kinetics.[18] In any case, the iCVD kinetic model developed earlier can now be quantitatively fitted to the experimental data in Figure 2.

Data Conversion. However, as a first step, the experimental data in Figure 2 needs to be converted to the variable forms with the appropriate dimensions used in the mathematical model prior to fitting. Because the model relates rate of polymerization, R_p, and number-average molecular weight, M_n, to monomer concentration, [M], this means P_M/P_{sat} has to be transformed to [M] in mol/L, while deposition rate has to be changed to R_p in mol/L·s. P_M/P_{sat} can be transformed through the use of the BET equation (eq 5), which yields an areal concentration, N_s, that can then be converted to a volume concentration, [M], by assuming that the adsorbed monomer molecules occupy a reaction volume having *a constant adlayer thickness equal to the monolayer thickness*, h_{ml}, an assumption that is expected to be applicable for all concentrations less than and up to a full monolayer coverage, i.e.:

$$[M] = \frac{N_s}{N_{av}h_{ml}} = \frac{\rho_M V_{ad}}{MW_M A_{QCM} h_{ml}} = \frac{\rho_M}{MW_M} \cdot \frac{V_{ad}}{V_{ml}} \qquad (6)$$

Relating V_{ad} back to P_M/P_{sat} with eq 5 enables the conversion to [M]. To obtain R_p from deposition rate, *DR*, a mass balance

is made between the amount of monomer consumed and the resulting polymer that is formed. Because R_p is by definition the rate of monomer disappearance, $-$d[M]/dt, while *DR* is the rate of increase in the thickness of polymer formed by conservation of mass, then:

$$\frac{R_p}{[M]} h_{ml} \rho_{ad} = DR \cdot \rho_p \text{ where } \rho_{ad} = MW_M[M] \qquad (7)$$

The left-hand side of eq 7 expresses the mass of monomer units consumed per unit area per unit time. Given that [M] is the amount of monomer within an adlayer of thickness h_{ml}, the ratio R_p/[M] represents the number of adlayers that have been consumed per unit time, while multiplying this ratio by the adlayer thickness, h_{ml}, and the adlayer monomer density, ρ_{ad}, yields the final monomer consumption rate per unit area. On the right-hand side of eq 7, multiplying DR by the polymer density, ρ_p ($= 1.08$ g/cm^3), gives the mass of monomer units formed into polymer per unit area per unit time. Simplifying eq 7 allows the conversion of *DR* to R_p:

$$R_p = \left(\frac{DR}{h_{ml}}\right)\left(\frac{\rho_p}{\rho_{ad}}\right)[M] = \frac{\rho_p DR}{h_{ml} MW_M} \qquad (8)$$

Equation 8 can be equivalently derived by considering that the ratio DR/h_{ml} represents the number of adlayers that formed into polymer per unit time, the ratio ρ_p/ρ_{ad} represents a correction for the volume change upon polymerization, and [M] is the monomer concentration within an adlayer.

Parameter Estimation. With eqs 6 and 8, the experimental data in Figure 2 were transformed to conform with the variables used in the kinetic model. These data points are plotted in Figure 4. The mathematical model, given by eqs 1−4, was then fitted to these experimental data. Because the model consists of two responses (R_p, M_n) with dissimilar variances and as a function of a common set of unknowns (k_i, k_p, k_t, k_t', k_t'', r, a), a multiresponse parameter estimation procedure based on a determinant criterion was suitably employed. The rationale for a determinant criterion was first set forth by Box and Draper,[30] and relevant details can be found in Bates and Watts.[31] Succinctly, this procedure aims to minimize the determinant $d = |\mathbf{Z}^T\mathbf{Z}|$, where $\mathbf{Z}$ is defined as:

$$\mathbf{Z}(\boldsymbol{\theta}) = \mathbf{Y} - \mathbf{H}(\boldsymbol{\theta}) \qquad (9)$$

with $\mathbf{Y}$ as an $N \times M$ matrix of N experimental observations for M responses and $\mathbf{H}$ as an $N \times M$ matrix of the corresponding model predictions based on P parameter estimates expressed collectively as $\boldsymbol{\theta}$. To minimize d, a Levenberg−Marquardt regularization algorithm[32−34] was used:

$$\boldsymbol{\theta}_{i+1} = \boldsymbol{\theta}_i - (\boldsymbol{\Omega} + \lambda \cdot \mathrm{diag}\Omega)^{-1}\boldsymbol{\omega} \qquad (10)$$

where $\boldsymbol{\omega}$ and $\boldsymbol{\Omega}$ are the gradient and Hessian matrices, respectively, of d with respect to $\boldsymbol{\theta}$ and evaluated at $\boldsymbol{\theta}_i$. λ is a dynamic scaling factor, which together with the diagonal of $\boldsymbol{\Omega}$, ensures that the Hessian matrix becomes positive definite, i.e., that d will have a minimum. With this iterative approach, on the basis of a multiresponse convergence criterion,[35] convergence is reached when:

$$\frac{||\mathbf{C}\boldsymbol{\delta}||^2/P}{2d/(N-P)} < \epsilon^2 \qquad (11)$$

where $\mathbf{C}$ is the Cholesky factor of the scaled $\boldsymbol{\Omega}$, $\boldsymbol{\delta}$ is equal to $(\boldsymbol{\theta}_{i+1} - \boldsymbol{\theta}_i)$, and ϵ is a prescribed tolerance, typically set at 0.001.

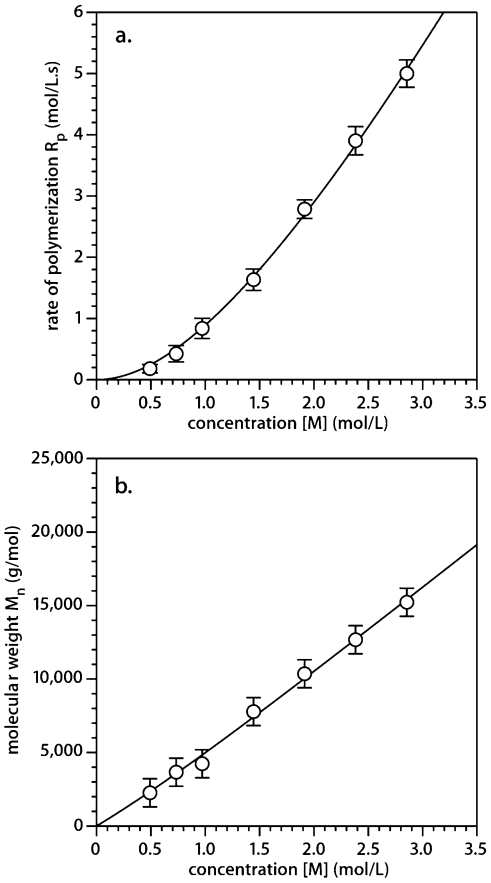

Figure 4. Comparison of the iCVD kinetic model to experimental data. Experimental data points were converted from Figure 2 to dimensions consistent with the model. The iCVD kinetic model of two responses (R_p, M_n), one fixed parameter (a) and six fitting parameters (r, k_i, k_p, k_t, k_t', and k_t'') was fitted to experimental data by using a multiresponse parameter estimation procedure with a determinant criterion that was minimized by a Levenberg−Marquardt routine. The model curve (for $a = 0.5$) matches closely with experiment, yielding a determinant minimum $d_{min} = 0.002\,161$ and a correlation coefficient $R^2 = 0.9972$. The resulting fitted parameter values are summarized in Table 2. The model captures the nonlinear polymerization rate behavior at low monomer concentrations as well as the linear rate and molecular weight behaviors typical of bulk-phase radical polymerization.

This determinant criterion multiresponse parameter estimation methodology was implemented by running a self-written code in Maple 9.5 (Maplesoft: Waterloo, Ontario, Canada), using full gradient and Hessian calculations.

In the present case, with seven measurements each for the two responses, $N = 7$ and $M = 2$. The number of fitting parameters in the model was reduced to six, i.e., $P = 6$, by setting the unknown a (defined in the model as the fraction of polymer radicals terminating by coupling) at a specific value. To facilitate convergence, matrix calculations were conditioned by scaling down M_n by a factor of 3000 so that their values and residuals were on the same order as that for R_p. Table 2 gives the optimized iCVD kinetic model parameters fitted to the experimental data, showing three different sets of fitted parameters obtained at values of $a = 0.0$, 0.5, and 1.0, their corresponding minimized determinants at convergence, d_{min}, and also their correlation coefficients, R^2. It can be seen that there are some variations in the fitted parameters for different values of a, although it can be argued that the variations are not huge, less than a factor of 2 or 3 between the extremes. Interestingly, both d_{min} and R^2 are the same across the three model fits, indicating that they all fit the experimental data equally well. However, because there is no a priori reasoning to suggest that

Table 2. iCVD Kinetic Model Parameters Fitted Using a Determinant Criterion for Multiresponse Parameter Estimation and Comparison with Literature

parameter[a]	model ($a = 0.0$)	model ($a = 0.5$)	model ($a = 1.0$)	literature[b]
r	0.083	0.110	0.165	
k_i	5720	4990	4820	
k_p	16 160	15 540	14 950	15 460
k_t	0.78×10^6	0.98×10^6	1.34×10^6	10^6
k_t'	8.21×10^7	6.89×10^7	6.40×10^7	
k_t''	13.0×10^8	7.41×10^8	4.60×10^8	3.98×10^8
	$d_{min} = 0.002\,161$	$d_{min} = 0.002\,161$	$d_{min} = 0.002\,161$	
	$R^2 = 0.9972$	$R^2 = 0.9972$	$R^2 = 0.9972$	

[a] r in mol/L·s; rate coefficients in L/mol·s. [b] k_p see ref 36; k_t see ref 37; k_t''see ref 38.

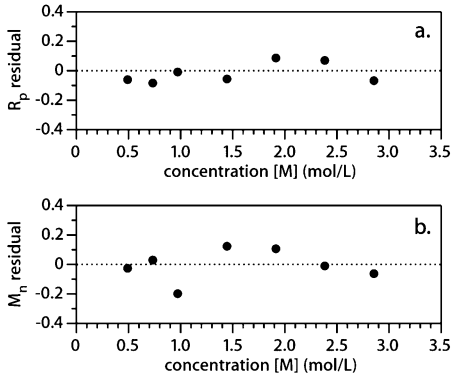

Figure 5. Residuals of R_p (a) and M_n (b) between the model (for $a = 0.5$) and experiment. M_n and its residuals have been scaled down by a factor of 3000 so that they are of the same order as for R_p and its residuals as a way to condition the model for convergence. Residuals show no systematic errors or bias, indicating a well-behaved model system.

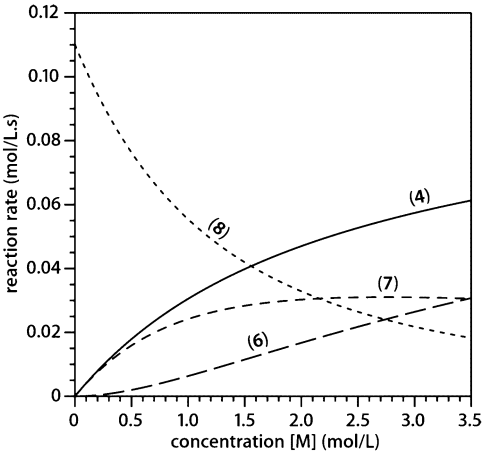

Figure 6. Reaction rate curves for initiation (**4**), bimolecular chain termination (**6**), primary radical termination (**7**), and primary radical recombination (**8**) derived from the fitted model (for $a = 0.5$). At low monomer concentrations, primary radical termination and recombination are significant, providing a possible explanation for the less-than-linear increase in polymerization rate because, without sufficient monomer, the primary radicals terminate chains prematurely, leading to shorter chains and slower polymerization. At high monomer concentrations, the initiation and chain termination rates improve, leading to the usual rate behavior expected for radical polymerization.

polymer radicals in an iCVD environment would preferentially terminate either by coupling or disproportionation, the discussion and assessment of the model which follows will be based on the fitting results at $a = 0.5$, i.e., bimolecular chain termination is assumed to be perfectly random. Nevertheless, the results at $a = 0.0$ and $a = 1.0$ represent the upper and lower bounds between which the actual value of each parameter will lie.

Model Analysis. Figure 4 plots the resulting model curves of R_p and M_n, using the fitted model parameters for $a = 0.5$. The curves match closely with the experimental data points of actual butyl acrylate iCVD polymerization from the controlled experiment of Table 1. The corresponding R_p and M_n residuals plotted in Figure 5 show that these residuals are randomly distributed, indicating that the model is well-behaved with no systematic error or bias, the correlation coefficient of the model being 0.9972. The agreement between model and experiment lends credible validity to the iCVD reaction mechanism of Figure 1 on which the model is derived, a mechanism that is surface-driven and subject to the amount of monomer adsorption and monomer surface concentration.

Interestingly, Table 2 reveals that the model propagation and termination rate coefficients, k_p and k_t of 15 540 and 0.98×10^6 L/mol·s, respectively, are quite close to the literature values from liquid-phase radical polymerization of butyl acrylate. The literature k_p was computed based on an Arrhenius equation obtained experimentally from butyl acrylate pulsed laser polymerization: $\ln[k_p\ (\text{L/mol·s})] = 16.71 - 2092/T(\text{K})$,[36] which at $T = 23$ °C has a value of 15 460 L/mol·s. With less reliable data on k_t, the literature k_t of $\sim 10^6$ L/mol·s was estimated based on experiments under different solvents and conditions.[37] The agreement between model and literature rate coefficients strongly implies that iCVD polymerization on a surface behaves almost identically as radical polymerization in a bulk medium. It is as if the surface was nonexistent, with no surface confinement or orientation effects that may influence reactivity.

More interestingly, primary radicals play a significant role in iCVD kinetics, at least within the range of process conditions considered here. The model rate coefficient of primary radical termination, k_t' of 6.89×10^7 L/mol·s, is significantly higher than k_t by nearly 2 orders of magnitude, and it simply reflects the greater ease with which smaller primary radicals can terminate a polymer radical compared with bulkier polymer radicals. The model primary radical recombination rate coefficient, $k_t''$of 7.41×10^8 L/mol·s, is within the range expected for small organic radicals (10^8−10^{10} L/mol·s). For example, the ethyl radical is reported to have a recombination rate coefficient of 3.98×10^8 L/mol·s with zero activation energy when measured in the gas phase.[38] As noted earlier, because the ethyl radical is believed to be the primary radical from the *tert*-amyl peroxide initiator, the model recombination rate coefficient may possibly correspond to ethyl radical recombination, the higher model value conceivably due to a denser environment on the surface compared to that of the gas phase. Recall that the ethyl radical is created through rapid β-scission of the peroxyl radical from the initial dissociation of *tert*-amyl peroxide i.e., $[(C_2H_5)(CH_3)_2CO\bullet \rightarrow C_2H_5\bullet + (CH_3)_2C{=}O]$.[19−21]

To look at the effect of primary radicals more closely, Figure 6 plots the rates of various surface reaction steps of the model, as described in Figure 1. Specifically, the rates of initiation (**4**), bimolecular chain termination (**6**), primary radical termination

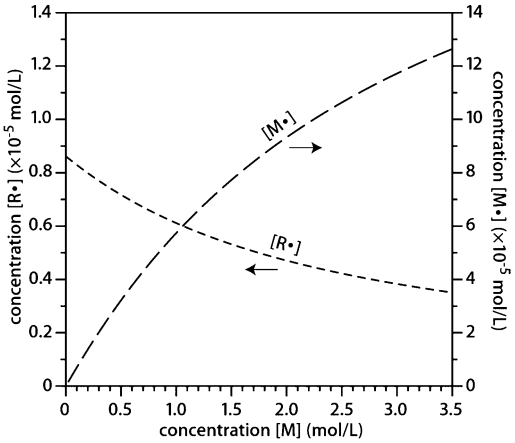

Figure 7. Concentration curves of primary radicals [R•] and polymer radicals [M•] derived from the fitted model (for $a = 0.5$). The higher primary radical concentration at low monomer concentrations that leads to the nonlinear polymerization rate is clearly evident. Radical concentrations are substantially (10^4-10^5) lower than monomer concentration, offering a reason iCVD kinetics tend to parallel that of bulk-phase radical polymerization because any surface effects that may influence radical reactivity would be negligible, as the radicals are essentially surrounded by monomer.

(**7**), and primary radical recombination (**8**) are shown as a function of monomer surface concentration. At low monomer concentrations, primary radical recombination and primary radical termination dominate, and with insufficient monomer to bring about appreciable initiation and propagation, polymer chains are shorter and there is a less than linear rate of polymerization, which is captured by the model, as seen in Figure 4. This behavior has been similarly observed in liquid-phase radical polymerization and is attributed to a higher concentration of primary radicals,[22,39,40] which this present model also attests to in Figure 6. At high monomer concentrations, normal bimolecular chain termination becomes substantial as does initiation when compared to the closure events involving primary radicals. This gives rise to linear polymerization rate and molecular weight dependencies that are analogous to the typical behavior in liquid-phase radical polymerization.[22]

Although the lower initiation rate coefficient, k_i of 4990 L/mol·s, when compared to the other rate coefficients seems to suggest that initiation may be fairly inefficient, the actual initiation rate from Figure 6 is comparable to the rates of the other reaction steps. This no doubt is due to its dependence on monomer surface concentration (**4**), which is considerably higher than either the primary radical or polymer radical concentrations, as Figure 7 reveals. The extremely low radical concentrations, 10^4-10^5 times lower than monomer concentration as Figure 7 shows, also mean that any influence of the surface on the reactivity of these radicals are expected to be negligible because these radicals are essentially surrounded by a "sea" of monomer molecules. Thus, it is perhaps not surprising to see that the derived model rate coefficients are similar to those of bulk-phase reactions, and that iCVD kinetics consistently display behaviors that parallel liquid-phase radical polymerization.

As Figure 6 points out, the model rate of primary radical "appearance", r of 0.110 mol/L·s, is in fact equal to the primary radical recombination rate when $[M] = 0$, i.e., when there is no polymerization, so as to satisfy the steady-state radical concentration assumption. Otherwise, it is difficult to comment on the value of r because, as discussed earlier, r may not be directly related to any physical process. Simply, r only refers to the rate of primary radicals adsorbed that eventually get consumed within the model reaction system of Figure 1. It does not reflect the overall rate of primary radical adsorption if there are radical sinks that scavenge off some of these radicals away from polymerization. It should be noted that, although r is expected to increase with an increase in initiator concentration following the experimental conditions of Table 1, r has been taken to be constant because experimental depositions with constant initiator concentration at a constant flow rate of 0.7 sccm (data not shown) did not show any rate differences compared with depositions in this study at the same monomer concentration. This just means that initiator levels are such that iCVD kinetics are zero order with respect to initiator concentration, which earlier iCVD reports have indicated.[2]

Table 3. iCVD Kinetic Model Parameter Variations for a Fixed Deviation of the Determinant Criterion from the Minimum ($d/d_{min} = 1.1$)

parameter[a]	(−) variation (%)	(+) variation (%)
a	3.12	3.06
r	1.57	1.62
k_i	1.35	1.37
k_p	0.66	0.66
k_t	2.27	2.31
k_t'	1.50	1.49
k_t''	5.74	5.69

[a] Single parameter variation as a percentage change from their model value (for $a = 0.5$) in either direction.

Model Sensitivity. Finally, local sensitivities of the model to variations in the model parameters have been determined. In terms of single parameter variations, Table 3 shows the change in either direction of each model parameter value that would cause an increase in the determinant criterion away from the minimum by 10% while keeping all other parameters unchanged. Model sensitivity to individual parameter variation can therefore be ranked as: $k_p > k_i \sim k_t' \sim r > k_t > a > k_t''$. It makes sense that changes in k_p would cause the largest shift from the optimum because it is the fundamental parameter in iCVD kinetics that determines both rate of polymerization and molecular weight. The fact that the model is more sensitive to a variation in k_t' than either k_t or k_t'' reflects the importance placed on primary radical termination in the final model solution. The model is relatively insensitive to changes in a and k_t'', not surprisingly because neither parameter contributes directly to polymerization reaction rates, with k_t'' determining only the rate of primary radical recombination and a defining to a certain extent the final distribution of chain lengths but having no influence on the rate of polymerization. In terms of two-parameter sensitivities, Figure 8 displays the contour plots of the determinant criterion surface around the minimum as a function of a simultaneous change in k_p and each of the six other parameters. Skewing of the contour lines away from the two orthogonal axes reveals any correlated effect between parameter pairs on model sensitivity. As such, a, r and k_t'' show minimal codependencies with k_p, while k_i and k_t' show significant correlation with k_p. Interestingly, variations of k_t' and k_p in the same direction results in less model deviation as is true for variations of k_i and k_p in opposite directions. This means that k_t' and k_p work in opposite ways, while k_i and k_p work in the same way in influencing rate behavior in a concerted manner, which is as expected. From these local sensitivity analyses, it appears that the effect of parameter variations on the model is in line with realistic trends anticipated for these parameters. This implies the model behaves well and the model parameter values are within a reasonable level of confidence.

Model Utility. With the ability to obtain validated model descriptions of iCVD kinetics, any developed model would

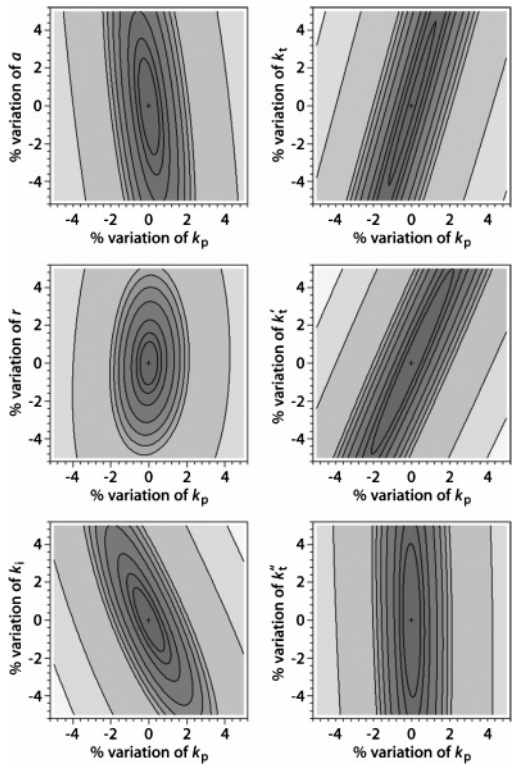

Figure 8. Two-parameter sensitivity plots showing the determinant criterion surface around the minimum for variations of k_p and each of the six other model parameters: a, r, k_i, k_t, k_t', and k_t'' by ±5% from their optimal values (for $a = 0.5$). Contour lines (where shown) are at 1.05, 1.1, 1.2, 1.4, 1.6, 1.8, 2.0, 5.0, and 10.0 times the determinant minimum. The plot with k_t has an additional contour at 1.01 times the minimum to show that the contours are not open-ended. Plots with k_i and k_t' give appreciable skewing of the determinant surface away from the two orthogonal axes, indicating significant correlation of these parameters with k_p in influencing model sensitivity. As alluded to in these plots, k_i and k_p work in the same direction, while k_t' and k_p work in opposite directions in influencing rate behavior.

potentially be useful as a tool to enable systematic scale-up of the iCVD process toward manufacturing, such as providing quantitative scaling laws, identifying important factors affecting rate and product quality, and highlighting possible physical limitations to scale-up. Perhaps more significantly, a better understanding of iCVD reaction pathways through kinetic modeling would provide valuable information toward determining a priori the feasibility of new iCVD chemistries. For example, the model presented here gives several criteria for iCVD viability. First, there must be appreciable adsorption of the monomer at the surface. This can be achieved by choosing heavier monomers with lower vapor pressures, although there is the additional constraint that the monomers must be volatile enough to be delivered into the iCVD reactor as a vapor. Alternatively, surface adsorption can be enhanced by lowering substrate temperature, although care must be taken to prevent monomer condensation. As mentioned in the preceding paper, a general rule of thumb is to operate within a P_M/P_{sat} range of 0.4−0.7 for optimal results.[18] Second, monomers should ideally have high kinetic coefficients of propagation to achieve appreciable deposition rates. Because propagation rate coefficients are similar to that of bulk-phase values, any reported data of the latter would be helpful in assessing polymerizability under iCVD conditions. Hence, acrylates and methacrylates will generally be more favorable compared to styrenes in iCVD polymerization.[37] Finally, with iCVD kinetics being susceptible to primary radical effects, attention must be given to ensure operability under process conditions where primary radical termination does not become dominating and hinder rates.

Conclusion

A mathematical model was developed to understand and explain the rate behavior of the iCVD process. Because the preceding paper found experimentally that iCVD polymerization is primarily surface-driven, an iCVD reaction mechanism was therefore formulated into a kinetic model that focused on surface events of initiation, propagation, and termination. The model also included primary radical termination and recombination, which can be important based on experimental observations. The model assumed a constant flux of primary radicals to the surface that took part in the iCVD surface reactions and further assumed a steady state concentration of primary and polymer radicals. In its final form, the model related the rate of polymerization and kinetic chain length to monomer surface concentration. This model was fitted to a set of butyl acrylate iCVD experimental data, which showed a linear increase in molecular weight with concentration and likewise in deposition rate at sufficiently high concentrations, while at low monomer concentrations, a deviation from linearity that was attributed to considerable primary radical termination. By using a multiresponse parameter estimation procedure with a determinant criterion that was minimized by a Levenberg−Marquardt algorithm, and based on two responses, one fixed parameter, and six fitting parameters, the model solution was able to describe the experimental trends closely, yielding a determinant minimum $d_{min} = 0.002\,161$ and a correlation coefficient $R^2 = 0.9972$. The model propagation and bimolecular chain termination rate coefficients, 15 540 and 0.98×10^6 L/mol·s, respectively, matched well with literature data from liquid-phase butyl acrylate radical polymerization, 15 460 and 10^6 L/mol·s, respectively. These results provided strong evidence for the similarities between iCVD and liquid-phase radical polymerization, indicating that the surface has practically no influence on kinetics, which was borne out by the much higher monomer concentration compared to radical concentrations and at a level comparable to liquid-phase concentrations such that rapid deposition rates can be achieved. Local one- and two-parameter sensitivity analysis gave further support to a well-behaved model and model parameters that trended realistically, giving additional confidence to the model solution. A valid iCVD kinetic model would enable a priori predictions on the viability of new iCVD chemistries as well as aid systematic scale-up of the process.

Acknowledgment. We thank the DuPont MIT Alliance for financial support. We especially thank Dr. John H. McMinn of DuPont Central Research & Development for helpful discussions.

References and Notes

(1) Lau, K. K. S.; Bico, J.; Teo, K. B. K.; Chhowalla, M.; Amaratunga, G. A. J.; Milne, W. I.; McKinley, G. H.; Gleason, K. K. *Nano Lett.* **2003**, *3*, 1701−1705.
(2) Mao, Y.; Gleason, K. K. *Langmuir* **2004**, *20*, 2484−2488.
(3) Chan, K.; Gleason, K. K. *Langmuir* **2005**, *21*, 8930−8939.
(4) Chan, K.; Gleason, K. K. *Chem. Vap. Deposition* **2005**, *11*, 437−443.
(5) Ma, M.; Mao, Y.; Gupta, M.; Gleason, K. K.; Rutledge, G. C. *Macromolecules* **2005**, *38*, 9742−9748.
(6) Gorham, W. F. *J. Polym. Sci., Part A: Polym. Chem.* **1966**, *1.4*, 3027−3039.
(7) Bartlett, B.; Buckley, L. J.; Godbey, D. J.; Schroeder, M. J.; Fontenot, C.; Eisinger, S. *J. Vac. Sci. Technol., B* **1999**, *17*, 90−94.
(8) Yasutake, M.; Hiki, S.; Andou, Y.; Nishida, H.; Endo, T. *Macromolecules* **2003**, *36*, 5974−5981.

(9) Yasutake, M.; Andou, Y.; Hiki, S.; Nishida, H.; Endo, T. *J. Polym. Sci., Part A: Polym. Chem.* **2004**, *42*, 2621−2630.
(10) Andou, Y.; Yasutake, M.; Jeong, J. M.; Nishida, H.; Endo, T. *Macromol. Chem. Phys.* **2005**, *206*, 1778−1783.
(11) Yasutake, M.; Andou, Y.; Hiki, S.; Nishida, H.; Endo, T. *Macromol. Chem. Phys.* **2004**, *205*, 492−499.
(12) Orihashi, Y.; Iwata, R.; Taniguchi, I.; Itaya, A. *Chem. Mater.* **1995**, *7*, 324−332.
(13) Hsieh, M.-D.; Zellers, E. T. *Sens. Actuators, B* **2002**, *82*, 287−296.
(14) Tamada, M.; Omichi, H.; Okui, N. *Thin Solid Films* **1995**, *260*, 168−173.
(15) Tamada, M.; Omichi, H.; Okui, N. *Thin Solid Films* **1995**, *268*, 18−21.
(16) Beach, W. F. *Macromolecules* **1978**, *11*, 72−76.
(17) Ganguli, S.; Agrawal, H.; Wang, B.; McDonald, J. F.; Lu, T. M.; Yang, G. R.; Gill, W. N. *J. Vac. Sci. Technol., A* **1997**, *15*, 3138−3142.
(18) Lau, K. K. S.; Gleason, K. K. *Macromolecules* **2006**, *39*, 3688−3694.
(19) Mekarbane, P. G.; Tabner, B. J. *Magn. Reson. Chem.* **1998**, *36*, 826−832.
(20) Mekarbane, P. G.; Tabner, B. J. *Macromolecules* **1999**, *32*, 3620−3625.
(21) Nakamura, T.; Busfield, W. K.; Jenkins, I. D.; Rizzardo, E.; Thang, S. H.; Suyama, S. *Macromolecules* **1997**, *30*, 2843−2847.
(22) Odian, G. In *Principles of Polymerization*, 4th ed.; John Wiley & Sons: Hoboken, NJ, 2004; pp 198−349.
(23) Buback, M.; Egorov, M.; Gilbert, R. G.; Kaminsky, V.; Olaj, O. F.; Russell, G. T.; Vana, P.; Zifferer, G. *Macromol. Chem. Phys.* **2002**, *203*, 2570−2582.
(24) Junkers, T.; Theis, A.; Buback, M.; Davis, T. P.; Stenzel, M. H.; Vana, P.; Barner-Kowollik, C. *Macromolecules* **2005**, *38*, 9497−9508.
(25) Allen, P. E. M.; Patrick, C. R. *Makromol. Chem.* **1961**, *47*, 154−167.
(26) Brunauer, S.; Emmett, P. H.; Teller, E. *J. Am. Chem. Soc.* **1938**, *60*, 309−319.
(27) Sauerbrey, G. *Z. Phys.* **1959**, *155*, 206−222.
(28) Afeefy, H. Y.; Liebman, J. F.; Stein, S. E. In *NIST Chemistry WebBook, NIST Standard Reference Database, Number 69*; Linstrom, P. J.; Mallard, W. G., Eds.; National Institute of Standards and Technology: Gaithersburg, MD, 2005; http://webbook.nist.gov.
(29) Atkins, P.; de Paula, J. In *Physical Chemistry*, 7th ed.; W. H. Freeman & Co.: New York, 2002; p 992.
(30) Box, G. E. P.; Draper, N. R. *Biometrika* **1965**, *52*, 355−365.
(31) Bates, D. M.; Watts, D. G. In *Nonlinear Regression Analysis and Its Applications*; John Wiley & Sons: New York, 1988; pp 134−167.
(32) Levenberg, K. *Q. Appl. Math.* **1944**, *2*, 164−168.
(33) Marquardt, D. *SIAM J. Appl. Math.* **1963**, *11*, 431−441.
(34) Nocedal, J.; Wright, S. J. In *Numerical Optimization*; Springer: New York, 1999; pp 262−265.
(35) Bates, D. M.; Watts, D. G. *SIAM J. Sci. Stat. Comput.* **1987**, *8*, 49−55.
(36) Beuermann, S.; Paquet, D. A.; McMinn, J. H.; Hutchinson, R. A. *Macromolecules* **1996**, *29*, 4206−4215.
(37) Kamachi, M.; Yamada, B. In *Polymer Handbook*, 4th ed.; Brandup, J., Immergut, E. H., Gulke, E. A., Eds.; John Wiley & Sons: New York, 2003; Vol. 1, pp II(77)−II(95).
(38) Hiatt, R.; Benson, S. W. *J. Am. Chem. Soc.* **1972**, *94*, 6886−6888.
(39) Yoshioka, M.; Otsu, T. *Macromolecules* **1992**, *25*, 559−562.
(40) Lebreton, P.; Boutevin, B. *J. Polym. Sci., Part A: Polym. Chem.* **2000**, *38*, 1834−1843.

MA0601621